

CP-violating effects of the neutral triple gauge couplings in $Z(\ell\ell)\gamma$ production at the LHC

Artur E. Semushin^{a,b,*}, Evgeny Yu. Soldatov^{a,†}, Anastasia S. Kurova^a

^aNational Research Nuclear University MEPhI, Moscow, Russia

^bA. Alikhanyan National Science Laboratory (Yerevan Physics Institute), Yerevan, Armenia

*E-mail: AESemushin@mephi.ru

†E-mail: EYSoldatov@mephi.ru

Abstract

The main goal of modern experiments in high-energy physics area is to find deviations from the Standard Model, the theoretical framework which describes data well but is expected to be extended to a more general theory. The anomalous coupling approach provides an opportunity to look for a wide range of new physics effects in different experimental signatures thanks to its model independence. In this work, the neutral triple gauge couplings are considered in $Z(\ell\ell)\gamma$ channel, and an effective field theory is used to parameterize these couplings in the Lagrangian. Neutral triple gauge couplings are triple interactions between Z bosons and photons, and some of them violate CP symmetry. This work presents a study of CP-sensitive variables in the aforementioned channel using special angular variables and matrix-element-based optimal observables. Based on these variables, expected limits on the coupling parameters are set for the conditions of Run II and Run III at LHC experiments, demonstrating the possibility of studying the CP-violation using a neutral triple gauge coupling approach and special CP-sensitive variables.

1 Introduction

Standard Model (SM) of elementary particle physics describes experimental results obtained during the last 50 years in high energy physics well, and no deviations from the SM (so-called new physics) have been found at the LHC during Run I and Run II [1]. This leads to the fact that direct experimental searches for new particles become less prospective in the absence of significant energy growth. On the other hand, there are indirect approaches, which look for new physics by studying interactions of currently known particles. Thus, the latter ones are more suitable for the Large hadron collider (LHC) Run III and Run IV conditions, since they provide a way to look for new physics at the energy scale beyond the accelerator constraints.

Search for anomalous couplings is an indirect, model-independent way to probe physics beyond the SM (BSM). It is based on looking for experimental events containing SM particles with anomalous kinematics compared to the SM predictions. This work studies neutral triple gauge couplings (nTGCs), which are forbidden in the SM at the tree level. Effective field theory (EFT) [2, 3] is used to parameterize these couplings in the Lagrangian. Free parameters of the EFT, Wilson coefficients, are usually constrained experimentally because of the absence of new physics manifestations. Setting such limits can provide the definition of the most likely region where the new physics is located, as well as the restriction of some SM extensions.

Anomalous couplings can violate CP symmetry and, therefore, a search for them can provide a model-independent probe of CP violation. Many experimental analyses study CP properties of the anomalous couplings [4, 5, 6, 7, 8]. In the case of nTGCs, the analyses usually focus their searches on the CP-conserving contributions and do not study CP violation [9, 10, 11, 12, 13, 14]. CP violation in the nTGC sector has been probed in ATLAS study of $ZZ(4\ell)$ production [15], where the limits on the anomalous coupling parameters have been set based on CP violating contributions. Moreover, CP-violating effects of nTGCs have been taken into account in L3 study of nTGCs based on the $Z\gamma$ production in e^+e^- collisions [16].

In this work, CP-violating nTGCs are studied using two kinds of special CP-sensitive variables. Reconstruction of such variables requires the presence of well-identified fermions in the final state. Therefore, for example, $Z(\nu\nu)\gamma$ production at the LHC, which has a high sensitivity to CP-conserving nTGC contributions, has no sensitivity to CP-violating ones. Thus, this work uses $Z(\ell\ell)\gamma$ production at the LHC for the sensitivity studies and comparison of the two variables.

2 Phenomenology of neutral triple gauge couplings

New physics, which includes new heavy particles at an experimentally inaccessible energy scale Λ , appears at low energies as anomalous couplings of already known particles. Such anomalous couplings can be parameterized in the Lagrangian by effective field theory (EFT) in the following way:

$$\mathcal{L} = \mathcal{L}_{\text{SM}} + \sum_{d>4} \mathcal{L}^{(d)}, \quad (1)$$

where \mathcal{L}_{SM} is dimension-four SM Lagrangian and $\mathcal{L}^{(d)}$ is dimension- d anomalous term. Each such term consists of a set of dimension- d operators $\mathcal{O}_i^{(d)}$ with corresponding Wilson coefficients:

$$\mathcal{L}^{(d)} = \sum_i \frac{C_i^{(d)}}{\Lambda^{d-4}} \mathcal{O}_i^{(d)}. \quad (2)$$

In the SM, the values of all the Wilson coefficients $C_i^{(d)}$ are zero. Experimentally, no non-zero values have been observed, but limits on the coefficients have been set. Wilson coefficients can

be matched to the parameters of new physics models [17, 18] and, therefore, experimental limits on the Wilson coefficients constrain the parameter space of such theories.

SM as well as operators of five, six, and seven dimensions do not contain nTGCs at the tree level. Thus, the description of such interactions mostly arises in dimension-eight EFT operators. This work studies CP-violating effects, therefore, only CP-odd operators are considered. There are five such operators defined as follows [19, 20]:

$$\mathcal{O}_{BW} = i\Phi^\dagger B_{\mu\nu} \hat{W}^{\mu\rho} \{D_\rho, D^\nu\} \Phi + \text{h.c.}, \quad (3)$$

$$\mathcal{O}_{BB} = i\Phi^\dagger B_{\mu\nu} B^{\mu\rho} \{D_\rho, D^\nu\} \Phi + \text{h.c.}, \quad (4)$$

$$\mathcal{O}_{WW} = i\Phi^\dagger \hat{W}_{\mu\nu} \hat{W}^{\mu\rho} \{D_\rho, D^\nu\} \Phi + \text{h.c.}, \quad (5)$$

$$\mathcal{O}_{\tilde{G}^+} = g^{-1} B_{\mu\nu} W^{\alpha\mu\rho} (D_\rho D_\lambda W^{\alpha\nu\lambda} + D^\nu D^\lambda W_{\lambda\rho}^\alpha), \quad (6)$$

$$\mathcal{O}_{\tilde{G}^-} = g^{-1} B_{\mu\nu} W^{\alpha\mu\rho} (D_\rho D_\lambda W^{\alpha\nu\lambda} - D^\nu D^\lambda W_{\lambda\rho}^\alpha). \quad (7)$$

These operators are constructed out of the SM fields and parameters: Φ , $B_{\mu\nu}$ and $\hat{W}_{\mu\nu}$ are the Higgs doublet, $U(1)$ and $SU(2)$ gauge field tensors respectively, g is the $SU(2)$ coupling constant, and D_μ is the covariant derivative.

The production of two neutral gauge bosons, such as ZZ or $Z\gamma$, is usually a basis for studying nTGCs because of their sensitivity to such BSM manifestations [21]. Example diagrams of this process, containing zero or one nTGCs, are presented in Figure 1. Squared matrix element of the process, containing up to one nTGC, in case of one non-zero Wilson coefficient, can be written in the following form:

$$|\mathcal{M}|^2 = |\mathcal{M}_{\text{SM}}|^2 + C/\Lambda^4 \cdot 2\text{Re} \mathcal{M}_{\text{SM}}^\dagger \mathcal{M}_{\text{BSM}}. \quad (8)$$

It consists of the SM term and interference (linear) term between SM-like and nTGC-like diagrams. The SM term is CP-conserving, whereas the interference term violates CP in the case of CP-violating operators. It should be emphasized that quadratic term is dropped in this work since it conserves CP. Additionally, the quadratic term at high sensitivity should be suppressed by the new physics energy scale ($\propto \Lambda^{-8}$) compared to the interference term.

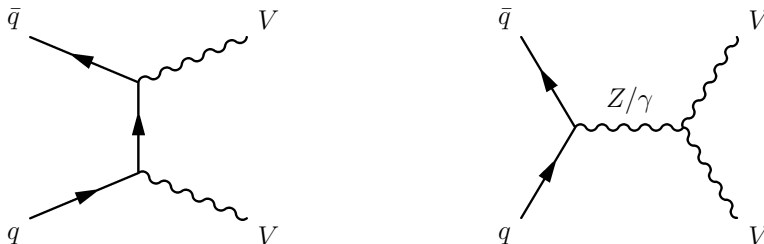


Figure 1: Feynman diagram examples for two neutral gauge boson production at the LHC. The left diagram is allowed by the SM, whereas the right one contains an nTGC.

After phase-space integration, CP-violating contribution is zero and does not affect a total process cross section. However, differential distributions by special CP-sensitive variables can significantly change. Such variables allow one to separate positive and negative effects of CP violation, and, therefore, are necessary for studies of CP-violating effects in nTGCs. This study uses $Z(\ell\ell)\gamma$ production as an example for variable construction and sensitivity study since it has a well-identified final state with fermions, which leads to a good CP sensitivity.

3 CP-sensitive variables

3.1 Angular variables

Simple angular CP-sensitive variables can be constructed using the direction of motion of Z boson decay products [22]. For this purpose, a special reference frame should be used. In order to simulate the decay of Z boson at rest, its rest frame is used. Z boson decay can be described by two angles θ and φ , and in this work they are polar and azimuthal angles of the direction of motion of the negatively charged lepton. These angles should be measured relative to the special coordinate system to be CP-sensitive, so the coordinate axes in the special reference frame are defined as follows. z -axis is set along the direction of motion of $Z(\ell\ell)$ system in the $Z(\ell\ell)\gamma$ rest frame. x -axis is set so that it lies on the reaction plane and its projection on the detector¹ z -axis has the same sign as new z -axis projection on the old z -axis. y -axis is totally defined by the z - and x -axes and set following the right-hand rule. Illustration of the special coordinate system is presented in Figure 2.

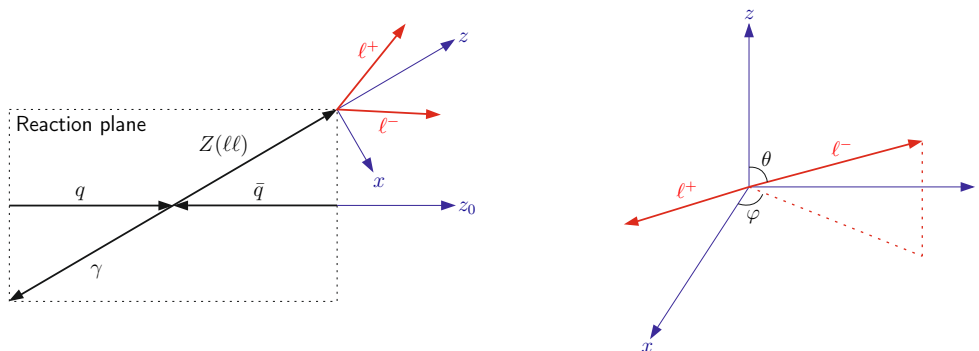


Figure 2: Scheme of the $Z(\ell\ell)\gamma$ production in the $Z(\ell\ell)\gamma$ rest frame with the new axes definitions (left), and CP-sensitive angle definitions in the $Z(\ell\ell)$ rest frame (right). In the left picture, all particles and axes lie on the reaction plane, excluding two leptons. The latter lie on the decay plane, which crosses the reaction plane along the z -axis. z_0 -axis in this picture is the conventional axis directed along the beam pipe.

In general, θ and φ are correlated, so they should be studied simultaneously to construct the CP-sensitive variable. Two-dimensional normalized distributions by these angles for SM and interference terms of two operators are presented in Figure 3. The SM contribution is positive in each bin, whereas SM-BSM interference has positive and negative parts. Localization of these parts at the two-dimensional angle distributions allows constructing the CP-sensitive variables, which separate positive and negative interference contributions. Thus, for coefficients C_{BB}/Λ^4 , C_{BW}/Λ^4 , C_{WW}/Λ^4 , and $C_{\tilde{G}_-}/\Lambda^4$, variable $\sin\varphi\cos\theta$ is used [15]. For coefficient $C_{\tilde{G}_+}/\Lambda^4$, the shape of a two-dimensional distribution is another, so a better separation power can be reached using another variable: $\sin 2\varphi$. The distributions of these variables can be found in Figure 4.

The aforementioned angular variables separate positive and negative interference contributions well, and their analyticity is their advantage. The regions of highest sensitivity of these variables are $|\sin\varphi\cos\theta| \gtrsim 0.2$ and $|\sin 2\varphi| \gtrsim 0.9$. Moreover, BSM contributions have another dependence on center-of-mass energy compared to the SM ones. Therefore, in order to reach better sensitivity to nTGCs, one should use a sensitive energetic variable in addition to the

¹Besides the special coordinate system for the study of CP violation, this work also uses a conventional for LHC experiments coordinate system. Its origin is at the center of the detector; x -, y - and z -axes are directed to the center of the LHC, upward and along the beam pipe respectively.

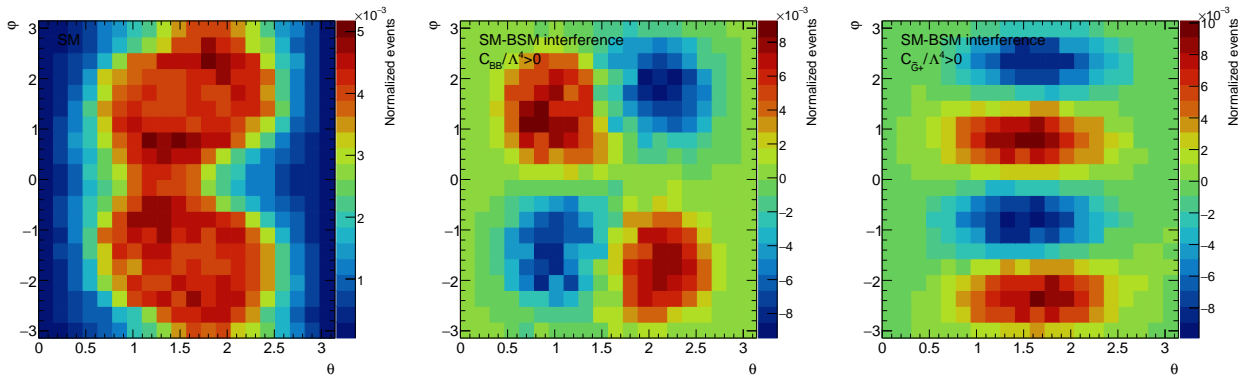


Figure 3: Normalized to unity two-dimensional distributions by CP-sensitive angles θ and φ : SM (left) and SM-BSM interference for C_{BB}/Λ^4 (center) and $C_{\tilde{G}_+}/\Lambda^4$ (right). Distributions for the other 3 coefficients are similar to the distribution for C_{BB}/Λ^4 . For the interference terms, the normalization is done using absolute values of the number of events in bins.

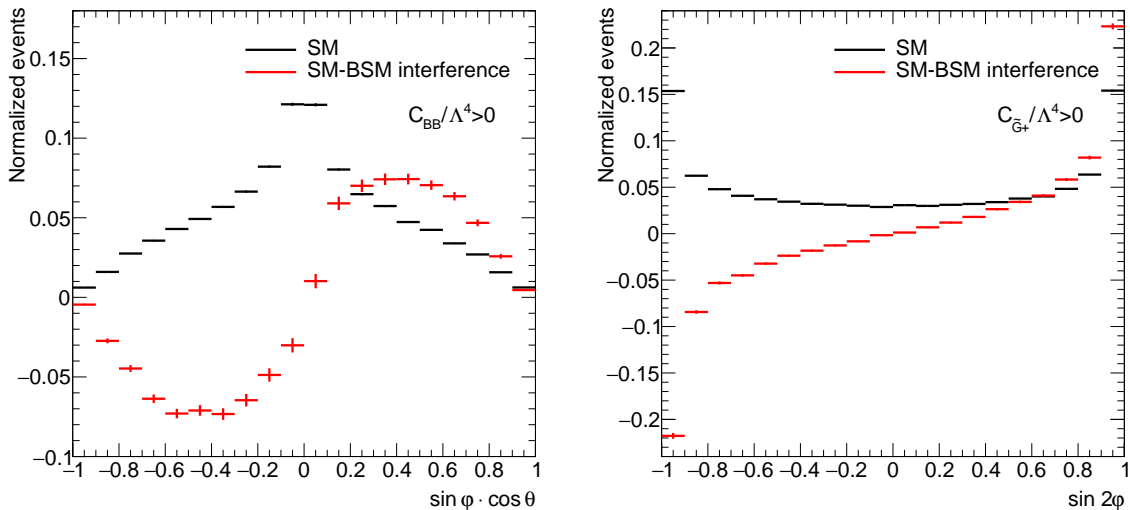


Figure 4: Normalized to unity distributions by CP-sensitive angular variables: $\sin \varphi \cos \theta$ for C_{BB}/Λ^4 (left) and $\sin 2\varphi$ for $C_{\tilde{G}_+}/\Lambda^4$ (right). For the interference terms, the normalization is done using absolute values of the number of events in bins.

angular CP-sensitive variable via e.g. cut or categorization. An example of nTGCs-sensitive energetic variable in $Z(\ell\ell)\gamma$ production is photon transverse momentum E_T^γ . Distributions by E_T^γ are shown in Figure 5 for the positive part of the interference terms. At high E_T^γ SM and interference contributions are well-separated and the sensitivity is the highest.

3.2 Optimal observables

The optimal observable technique [23, 24, 25] provides another way to construct the CP-sensitive variables. CP-sensitive optimal observable can be defined as the ratio of interference and SM parts of the process squared amplitude from Equation (8):

$$OO = \frac{2\text{Re } \mathcal{M}_{\text{SM}}^\dagger \mathcal{M}_{\text{BSM}}}{|\mathcal{M}_{\text{SM}}|^2}. \quad (9)$$

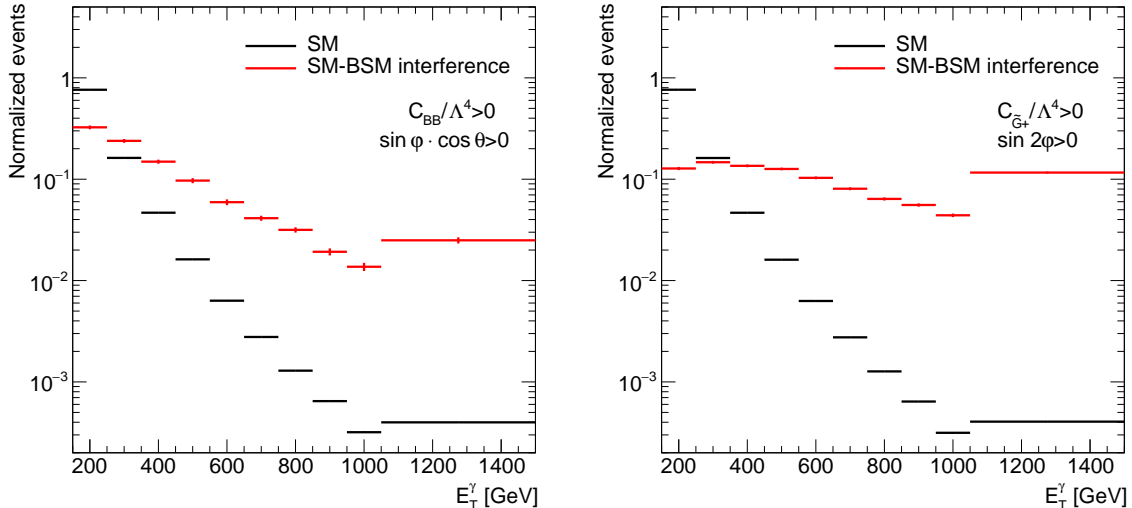


Figure 5: Normalized to unity distributions by photon transverse energy for SM and interference terms for C_{BB}/Λ^4 (left) and $C_{\tilde{G}_+}/\Lambda^4$ (right). Requirements $\sin \varphi \cos \theta > 0$ (left) and $\sin 2\varphi > 0$ (right) are applied to the distributions so that the interference term is positive. The last bin includes all overflow events.

Such a definition can be understood as a likelihood ratio. Thus, such a variable is expected to have perfect sensitivity to nTGCs, combining sensitivity from CP-sensitive angular variables and energetic ones in the most optimal way. The optimal observable method was used in the nTGC study by the L3 collaboration [16].

For the pp collisions, components of optimal observable should be calculated using parton matrix elements $\mathcal{M}_{\text{SM}}^{ij}$ and $\mathcal{M}_{\text{BSM}}^{ij}$:

$$2\text{Re } \mathcal{M}_{\text{SM}}^\dagger \mathcal{M}_{\text{BSM}} = \sum_{i,j} f_i(x_1, Q^2) f_j(x_2, Q^2) 2\text{Re } \mathcal{M}_{\text{SM}}^{ij \dagger} \mathcal{M}_{\text{BSM}}^{ij}, \quad (10)$$

$$|\mathcal{M}_{\text{SM}}|^2 = \sum_{i,j} f_i(x_1, Q^2) f_j(x_2, Q^2) |\mathcal{M}_{\text{SM}}^{ij}|^2, \quad (11)$$

where i, j are initial-state partons, $f_i(x, Q^2)$ is density function of parton i which depends on collinear momentum fraction x and factorization scale Q . Collinear momentum fractions of partons coming from positive and negative LHC z -axis directions can be reconstructed as

$$x_1 = \frac{m_{\ell\ell\gamma}}{\sqrt{s}} e^{y_{\ell\ell\gamma}}, \quad (12)$$

$$x_2 = \frac{m_{\ell\ell\gamma}}{\sqrt{s}} e^{-y_{\ell\ell\gamma}}, \quad (13)$$

where \sqrt{s} is pp center-of-mass energy, $m_{\ell\ell\gamma}$ and $y_{\ell\ell\gamma}$ are invariant mass and rapidity of the $\ell\ell\gamma$ system. The choice of the factorization scale depends on its definition in the matrix-element-level Monte Carlo event generator which is used to produce the events with non-zero Wilson coefficients. In this work, it is set to half of the sum of final particle transverse masses.

Optimal observable distributions for two operators are presented in Figure 6. These variables allow one to reach the perfect sensitivity to nTGCs, especially at the left and right tails of the distributions. It should be emphasized that each operator has its own optimal observable. ROC curves for angular variables, photon transverse energy and optimal observables are presented in Figures 7 and 8 for low and high photon transverse energies respectively. They are created using

the part of the distributions, where the interference term is positive. It can be seen that the performance of the optimal observable is the best. Angular variables show low sensitivity and are useful mainly for separation of positive and negative CP-violating contributions. Photon transverse energy has good sensitivity and is convenient to be used along with angular variables. Thus, nTGC limits based on the optimal observables are expected to be the most stringent.

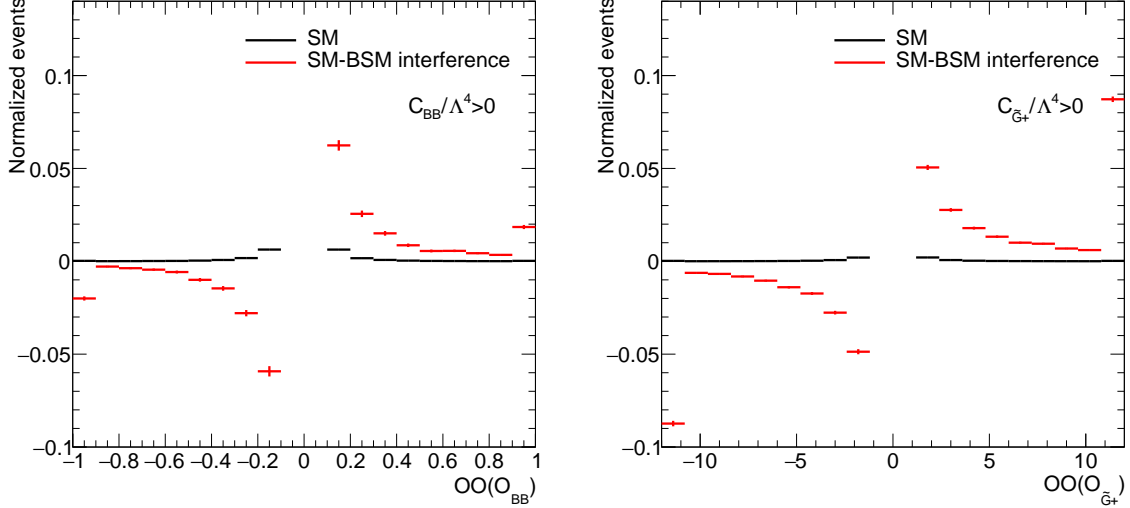


Figure 6: Normalized to unity distributions by CP-sensitive optimal observables for C_{BB}/Λ^4 (left) and $C_{\tilde{G}^+}/\Lambda^4$ (right). For the interference terms, the normalization is done using absolute values of the number of events in bins. Contents of two center bins are out of the plot range. The first and last bins include all underflow and overflow events correspondingly.

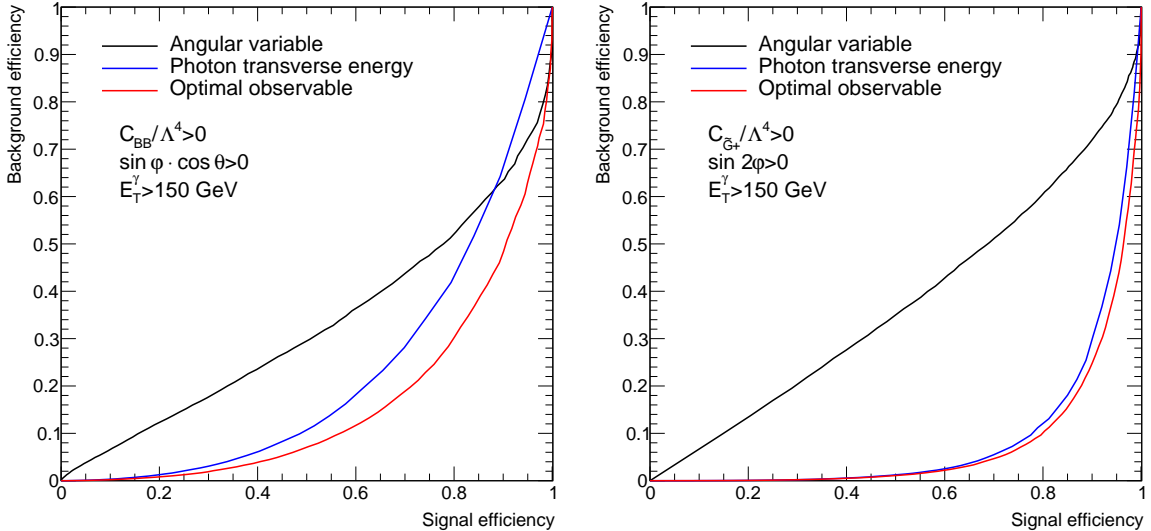


Figure 7: ROC curves for C_{BB}/Λ^4 at $\sin \varphi \cos \theta > 0$, $E_T^\gamma > 150$ GeV (left) and $C_{\tilde{G}^+}/\Lambda^4$ at $\sin 2\varphi > 0$, $E_T^\gamma > 150$ GeV (right). E_T^γ threshold is explained further in the text.

4 Sensitivity study for $Z(\ell\ell)\gamma$ production

In order to study the sensitivity of $Z(\ell\ell)\gamma$ production to CP-violating effects of nTGCs, expected limits on five Wilson coefficients are calculated. The phase-space region used in this

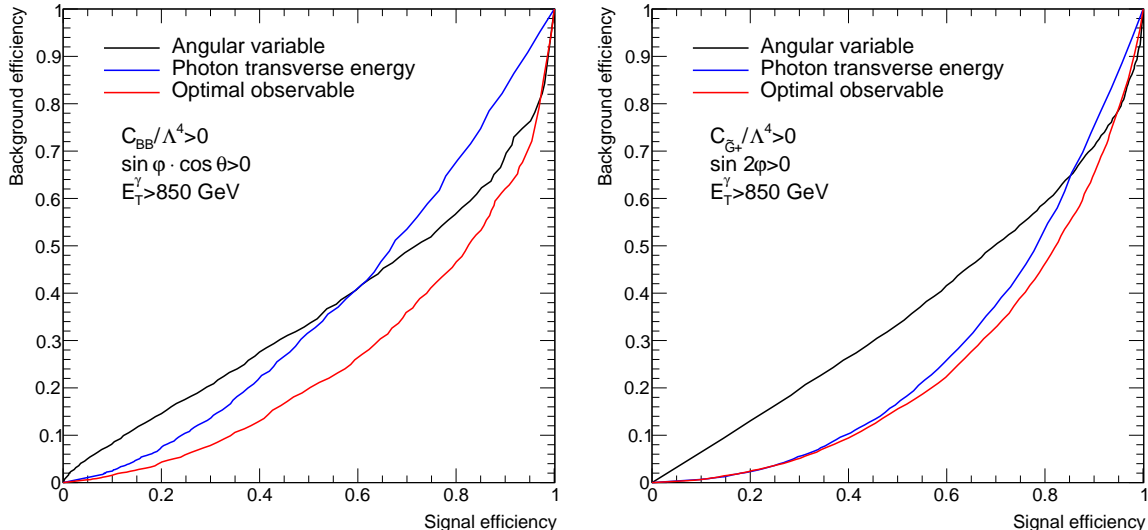


Figure 8: ROC curves for C_{BB}/Λ^4 at $\sin \varphi \cos \theta > 0$, $E_T^\gamma > 850$ GeV (left) and C_{G^+}/Λ^4 at $\sin 2\varphi > 0$, $E_T^\gamma > 850$ GeV (right). E_T^γ threshold is explained further in the text.

work is taken from the study of $Z(\ell\ell)\gamma$ production at LHC Run II by the ATLAS Collaboration [26], the main event selection criteria are summarized in Table 1. The additional criterion of $E_T^\gamma > 150$ GeV is added similarly to ATLAS studies of $Z\gamma$ production [13, 27], since low-energy contributions have negligible sensitivity to nTGCs. In this phase-space region, $Z(\ell\ell)\gamma$ production has some backgrounds which contamination is taken flat and equal to 18% of the signal process SM event yield in accordance with the aforementioned study [26].

Table 1: Event selection criteria for the sensitivity study.

1 opposite-charge same-flavor pair of leptons
1 photon
$p_T^{\ell_{\text{leading}}} > 30$ GeV, $p_T^{\ell_{\text{subleading}}} > 25$ GeV
$E_T^\gamma > 150$ GeV
$m_{\ell\ell} > 40$ GeV, $m_{\ell\ell\gamma} > 182$ GeV

Events of $Z(\ell\ell)\gamma$ production in pp collisions were generated using Monte Carlo event generator `MadGraph5_aMC@NLO` [28]. SM and SM-BSM interference contributions were modeled separately to obtain the decomposed resulting samples. In order to improve the Monte Carlo statistics, events were generated separately by slices in photon transverse energy: $150 < E_T^\gamma < 300$ GeV, $300 < E_T^\gamma < 600$ GeV, and $E_T^\gamma > 600$ GeV. Universal FeynRules Output model [29] including SM and CP-violating nTGC operators was created in `FeynRules` package [30] and used in the event generator. `Pythia8` [31] was used to model the parton shower, hadronization and underlying event, and `Delphes3` [32] simulated the response of the ATLAS detector [33] as an example of a typical detector at the LHC in this work. Matrix elements for optimal observables were calculated using standalone output in `MadGraph5_aMC@NLO`. For both event generation and optimal observable computation parton density function set `NNPDF30_nlo_as_0118` by NNPDF Collaboration [34] was used via `LHAPDF` tool [35].

The limits on the Wilson coefficients are set using the frequentist approach with likelihood-ratio-based test statistic, assuming its asymptotic distribution [36, 37]. The likelihood is constructed using distributions presented in Figures 9 and 10 for angular variables and in Figure 11 for optimal observables. Distributions by angular variables are split in six bins, and two categories depending on E_T^γ are used to improve the sensitivity. Distributions by optimal

observables are split in eight bins. The optimization study is performed to ensure that more bins or categories do not lead to a significant increase of the sensitivity. The positions of the last bin for both variables as well as the threshold, separating categories, are set to reach the best experimental sensitivity. The following E_T^γ thresholds between categories are set: 850 GeV for $C_{\tilde{G}_+}/\Lambda^4$, C_{BB}/Λ^4 and C_{BW}/Λ^4 ; 800 GeV for $C_{\tilde{G}_-}/\Lambda^4$; 900 GeV for C_{WW}/Λ^4 .

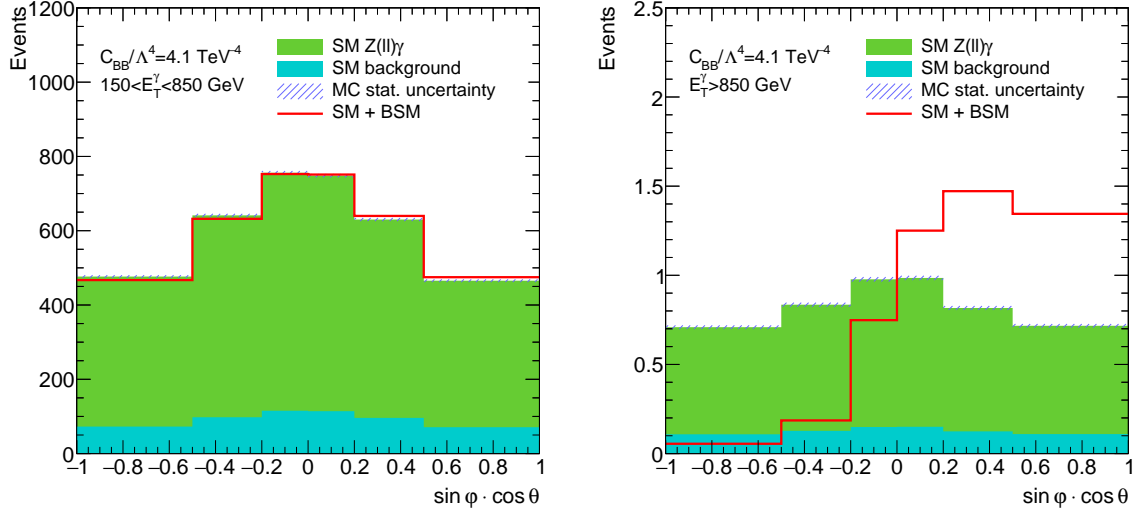


Figure 9: Distribution by $\sin \varphi \cos \theta$ for low-energy (left) and high-energy (right) slices. The case of Run II integrated luminosity is presented. The dashed band shows the statistical uncertainty of MC modeling. The same distributions are used for C_{BW}/Λ^4 , C_{WW}/Λ^4 , and $C_{\tilde{G}_-}/\Lambda^4$ coefficients.

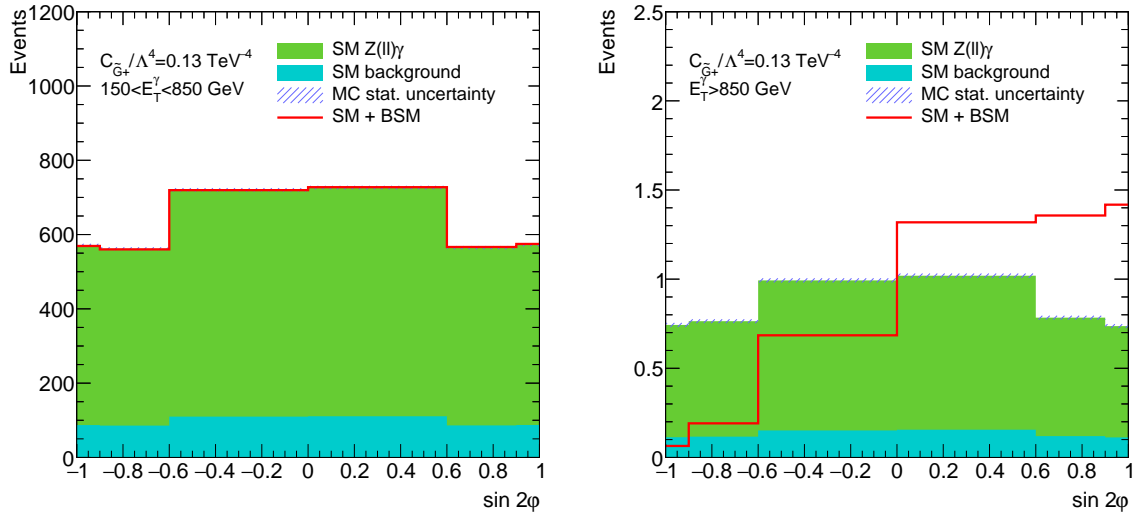


Figure 10: Distribution by $\sin 2\varphi$ for low-energy (left) and high-energy (right) slices. The case of Run II integrated luminosity is presented. The dashed band shows the statistical uncertainty of MC modeling.

In addition to the MC statistical uncertainty of the process modeling, the additional systematic uncertainty of 10% is added to the limit-setting procedure. Overall systematic uncertainties, which affect normalization only, do not have an impact on the resulting limits because of zero normalization of the CP-violating interference terms. Thus, additional systematic uncertainty is taken uncorrelated between bins, i.e. affecting both normalization and shape,

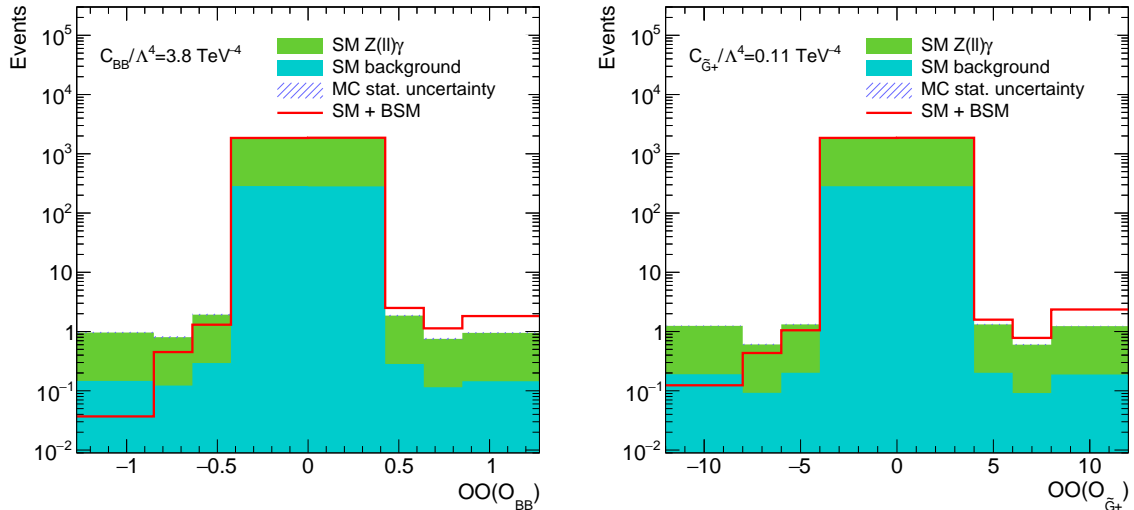


Figure 11: Distribution by optimal observable for C_{BB}/Λ^4 (left) and $C_{\tilde{G}_+}/\Lambda^4$ (right). The case of Run II integrated luminosity is presented. Dashed band shows the statistical uncertainty of MC modeling.

and is expected to approximately estimate theoretical and experimental systematic uncertainties [38, 26]. The resulting limits on five Wilson coefficients set basing on the angular variable and the optimal observable for LHC Run II and projected Run III integrated luminosities are presented in Table 2. The impact of the aforementioned systematic uncertainty on the limits is of 3–13% depending on coefficient, variable and luminosity. Optimal observables result in more stringent limits on CP-violating contributions of nTGCs. It should be emphasized that the optimization of binnings and threshold is done for the Run II conditions, therefore it is possible to improve the sensitivity for the Run III conditions after the reoptimization.

Table 2: Expected limits [TeV^{-4}] on five Wilson coefficients set basing on CP-sensitive angular variables and optimal observables for Run II and expected Run III integrated luminosities.

Coef.	140 fb^{-1}		300 fb^{-1}	
	Ang. var.	Opt. obs.	Ang. var.	Opt. obs.
C_{BB}/Λ^4	[-4.2; 4.1]	[-3.9; 3.8]	[-3.3; 3.2]	[-3.0; 3.0]
C_{BW}/Λ^4	[-9.2; 8.1]	[-7.8; 7.4]	[-7.1; 6.4]	[-6.1; 5.8]
C_{WW}/Λ^4	[-22; 21]	[-20; 19]	[-18; 17]	[-15; 15]
$C_{\tilde{G}_+}/\Lambda^4$	[-0.13; 0.13]	[-0.11; 0.11]	[-0.10; 0.10]	[-0.089; 0.090]
$C_{\tilde{G}_-}/\Lambda^4$	[-30; 33]	[-12; 12]	[-23; 25]	[-9.2; 9.0]

5 Conclusion

This work studies CP-violating contributions of neutral triple gauge couplings at the LHC, using $Z(\ell\ell)\gamma$ production as an example. Often, the LHC experiments do not study CP-violating contributions and base their analyses on the CP-conserving contributions. CP violation can be probed using interference between CP-violating BSM physics and the SM one. Pure BSM quadratic contributions can lead to significant improvement of the sensitivity, but do not allow studying CP violation because of their CP-conserving nature, and, thus, are not used in this work. Thus, this study shows an additional way to probe new physics in the nTGC sector and improve the limits.

CP-violating contributions were studied using two types of CP-sensitive variables: angular variables and an optimal observable. The angular observable $\sin\varphi\cos\theta$, measured for the negative lepton in a special reference frame, was shown to have good CP-sensitivity to Wilson coefficients C_{BB}/Λ^4 , C_{BW}/Λ^4 , C_{WW}/Λ^4 , and $C_{\tilde{G}_-}/\Lambda^4$. For coefficient $C_{\tilde{G}_+}/\Lambda^4$, more appropriate variable is $\sin 2\varphi$. Usage of such angular variables requires application of additional energetic variables to increase the sensitivity. At the same time, it was shown that optimal observables provide a way to combine angular CP-sensitive and energetic variables into a powerful variable with the perfect sensitivity to nTGCs. Expected limits on five Wilson coefficients were set in this work, using only CP-violating contributions of nTGCs in $Z(\ell\ell)\gamma$ production. Limits based on the optimal observables are 8–63% more stringent than the ones based on the angular variables with additional categorization in the energetic variable. Despite the fact that experimental limits, based on CP-conserving contributions, are basically more stringent than the ones based on CP-violating contributions [15], the increase of the luminosity provides more sensitivity and, therefore, the ratio of the interference and quadratic term contributions rises. Therefore, it is possible to set more stringent limits by combining variables, sensitive to CP-violating and CP-conserving contributions. Such a study can be applied to other channels, which has a sensitivity to CP violation. Finally, it can be important at ee colliders, such as CEPC [39] and ILC [40], which have lower center-of-mass energy, and where the interference term dominates over the CP-conserving quadratic one.

Acknowledgements

The work was funded by the Ministry of Science and Higher Education of the Russian Federation, Project "New Phenomena in Particle Physics and the Early Universe" FSWU-2023-0073.

References

- [1] PARTICLE DATA GROUP collaboration, *Review of particle physics*, *Phys. Rev. D* **110** (2024) 030001.
- [2] S. Weinberg, *Phenomenological Lagrangians*, *Physica A* **96** (1979) 327.
- [3] C. Degrande, N. Greiner, W. Kilian, O. Mattelaer, H. Mebane, T. Stelzer et al., *Effective Field Theory: A Modern Approach to Anomalous Couplings*, *Annals Phys.* **335** (2013) 21 [1205.4231].
- [4] ATLAS collaboration, *Test of CP invariance in vector-boson fusion production of the Higgs boson in the $H\rightarrow\tau\tau$ channel in proton–proton collisions at $\sqrt{s}=13\text{TeV}$ with the ATLAS detector*, *Phys. Lett. B* **805** (2020) 135426 [2002.05315].
- [5] ATLAS collaboration, *Test of CP Invariance in Higgs Boson Vector-Boson-Fusion Production Using the $H\rightarrow\gamma\gamma$ Channel with the ATLAS Detector*, *Phys. Rev. Lett.* **131** (2023) 061802 [2208.02338].
- [6] ATLAS collaboration, *Measurement of the polarisation of single top quarks and antiquarks produced in the t -channel at $\sqrt{s} = 13 \text{ TeV}$ and bounds on the tWb dipole operator from the ATLAS experiment*, *JHEP* **11** (2022) 040 [2202.11382].
- [7] ATLAS collaboration, *Test of CP-invariance of the Higgs boson in vector-boson fusion production and in its decay into four leptons*, *JHEP* **05** (2024) 105 [2304.09612].

- [8] CMS collaboration, *Constraints on anomalous Higgs boson couplings from its production and decay using the WW channel in proton–proton collisions at $\sqrt{s} = 13$ TeV*, *Eur. Phys. J. C* **84** (2024) 779 [2403.00657].
- [9] CDF collaboration, *Limits on Anomalous Trilinear Gauge Couplings in $Z\gamma$ Events from $p\bar{p}$ Collisions at $\sqrt{s} = 1.96$ TeV*, *Phys. Rev. Lett.* **107** (2011) 051802 [1103.2990].
- [10] D0 collaboration, *$Z\gamma$ production and limits on anomalous $ZZ\gamma$ and $Z\gamma\gamma$ couplings in $p\bar{p}$ collisions at $\sqrt{s} = 1.96$ TeV*, *Phys. Rev. D* **85** (2012) 052001 [1111.3684].
- [11] CMS collaboration, *Measurement of the $Z\gamma \rightarrow \nu\bar{\nu}\gamma$ production cross section in pp collisions at $\sqrt{s} = 8$ TeV and limits on anomalous $ZZ\gamma$ and $Z\gamma\gamma$ trilinear gauge boson couplings*, *Phys. Lett. B* **760** (2016) 448 [1602.07152].
- [12] ATLAS collaboration, *Measurement of ZZ production in the $\ell\nu\nu$ final state with the ATLAS detector in pp collisions at $\sqrt{s} = 13$ TeV*, *JHEP* **10** (2019) 127 [1905.07163].
- [13] ATLAS collaboration, *Measurement of the $Z\gamma \rightarrow \nu\bar{\nu}\gamma$ production cross section in pp collisions at $\sqrt{s} = 13$ TeV with the ATLAS detector and limits on anomalous triple gauge-boson couplings*, *JHEP* **12** (2018) 010 [1810.04995].
- [14] CMS collaboration, *Measurement of the inclusive and differential WZ production cross sections, polarization angles, and triple gauge couplings in pp collisions at $\sqrt{s} = 13$ TeV*, *JHEP* **07** (2022) 032 [2110.11231].
- [15] ATLAS collaboration, *Evidence of pair production of longitudinally polarised vector bosons and study of CP properties in $ZZ \rightarrow 4\ell$ events with the ATLAS detector at $\sqrt{s} = 13$ TeV*, *JHEP* **12** (2023) 107 [2310.04350].
- [16] L3 collaboration, *Study of the $e^+e^- \rightarrow Z\gamma$ process at LEP and limits on triple neutral-gauge-boson couplings*, *Phys. Lett. B* **597** (2004) 119 [hep-ex/0407012].
- [17] G.N. Remmen and N.L. Rodd, *Consistency of the Standard Model Effective Field Theory*, *JHEP* **12** (2019) 032 [1908.09845].
- [18] J. Ellis, H.-J. He, R.-Q. Xiao, S.-P. Zeng and J. Zheng, *UV Completion of Neutral Triple Gauge Couplings*, [2408.12508](#).
- [19] C. Degrande, *A basis of dimension-eight operators for anomalous neutral triple gauge boson interactions*, *JHEP* **02** (2014) 101 [1308.6323].
- [20] J. Ellis, H.-J. He and R.-Q. Xiao, *Probing neutral triple gauge couplings with $Z^*\gamma$ ($\nu\nu\bar{\gamma}$) production at hadron colliders*, *Phys. Rev. D* **108** (2023) L111704 [2308.16887].
- [21] A. Biekötter, P. Gregg, F. Krauss and M. Schönherr, *Constraining CP violating operators in charged and neutral triple gauge couplings*, *Phys. Lett. B* **817** (2021) 136311 [2102.01115].
- [22] D. Chang, W.-Y. Keung and P.B. Pal, *CP violation in the cubic coupling of neutral gauge bosons*, *Phys. Rev. D* **51** (1995) 1326 [hep-ph/9407294].
- [23] M. Diehl and O. Nachtmann, *Optimal observables for measuring three gauge boson couplings in $e^+e^- \rightarrow W^+W^-$* , in *Physics with e^+e^- Linear Colliders (The European Working Groups 4 Feb - 1 Sep 1995: Session 2)*, pp. 301–304, 3, 1996 [hep-ph/9603207].

- [24] N.L. Belyaev and E.Y. Soldatov, *Optimal observables as a probe of CP violation in the $q\bar{q} \rightarrow Z\gamma \rightarrow \nu\bar{\nu}\gamma$ process*, *J. Phys. Conf. Ser.* **1690** (2020) 012168.
- [25] S. Jahedi and J. Lahiri, *Probing anomalous $ZZ\gamma$ and $Z\gamma\gamma$ couplings at the e^+e^- colliders using optimal observable technique*, *JHEP* **04** (2023) 085 [[2212.05121](#)].
- [26] ATLAS collaboration, *Measurement of the $Z(\rightarrow \ell^+\ell^-)\gamma$ production cross-section in pp collisions at $\sqrt{s} = 13$ TeV with the ATLAS detector*, *JHEP* **03** (2020) 054 [[1911.04813](#)].
- [27] ATLAS collaboration, *Measurement of electroweak $Z(\nu\bar{\nu})\gamma jj$ production and limits on anomalous quartic gauge couplings in pp collisions at $\sqrt{s} = 13$ TeV with the ATLAS detector*, *JHEP* **06** (2023) 082 [[2208.12741](#)].
- [28] J. Alwall, R. Frederix, S. Frixione, V. Hirschi, F. Maltoni, O. Mattelaer et al., *The automated computation of tree-level and next-to-leading order differential cross sections, and their matching to parton shower simulations*, *JHEP* **07** (2014) 079 [[1405.0301](#)].
- [29] C. Degrande, C. Duhr, B. Fuks, D. Grellscheid, O. Mattelaer and T. Reiter, *UFO - The Universal FeynRules Output*, *Comput. Phys. Commun.* **183** (2012) 1201 [[1108.2040](#)].
- [30] A. Alloul, N.D. Christensen, C. Degrande, C. Duhr and B. Fuks, *FeynRules 2.0 - A complete toolbox for tree-level phenomenology*, *Comput. Phys. Commun.* **185** (2014) 2250 [[1310.1921](#)].
- [31] T. Sjöstrand, S. Ask, J.R. Christiansen, R. Corke, N. Desai, P. Ilten et al., *An introduction to PYTHIA 8.2*, *Comput. Phys. Commun.* **191** (2015) 159 [[1410.3012](#)].
- [32] DELPHES 3 collaboration, *DELPHES 3, A modular framework for fast simulation of a generic collider experiment*, *JHEP* **02** (2014) 057 [[1307.6346](#)].
- [33] ATLAS collaboration, *The ATLAS Experiment at the CERN Large Hadron Collider*, *JINST* **3** (2008) S08003.
- [34] NNPDF collaboration, *Parton distributions for the LHC Run II*, *JHEP* **04** (2015) 040 [[1410.8849](#)].
- [35] A. Buckley, J. Ferrando, S. Lloyd, K. Nordström, B. Page, M. Rüfenacht et al., *LHAPDF6: parton density access in the LHC precision era*, *Eur. Phys. J. C* **75** (2015) 132 [[1412.7420](#)].
- [36] S.S. Wilks, *The Large-Sample Distribution of the Likelihood Ratio for Testing Composite Hypotheses*, *Annals Math. Statist.* **9** (1938) 60.
- [37] G. Cowan, K. Cranmer, E. Gross and O. Vitells, *Asymptotic formulae for likelihood-based tests of new physics*, *Eur. Phys. J. C* **71** (2011) 1554 [[1007.1727](#)].
- [38] ATLAS collaboration, *Measurements of $Z\gamma$ and $Z\gamma\gamma$ production in pp collisions at $\sqrt{s} = 8$ TeV with the ATLAS detector*, *Phys. Rev. D* **93** (2016) 112002 [[1604.05232](#)].
- [39] CEPC STUDY GROUP collaboration, *CEPC Technical Design Report: Accelerator, Radiat. Detect. Technol. Methods* **8** (2024) 1 [[2312.14363](#)].
- [40] T. Behnke, J.E. Brau, B. Foster, J. Fuster, M. Harrison, J.M. Paterson et al., eds., *The International Linear Collider Technical Design Report - Volume 1: Executive Summary*, [1306.6327](#).